

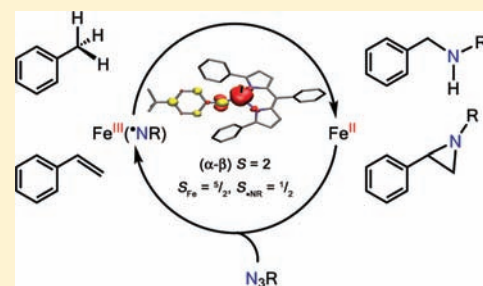
Catalytic C–H Bond Amination from High-Spin Iron Imido Complexes

Evan R. King, Elisabeth T. Hennessy, and Theodore A. Betley*

Department of Chemistry and Chemical Biology, Harvard University, 12 Oxford Street, Cambridge, Massachusetts 02138, United States

Supporting Information

ABSTRACT: Dipyrrromethene ligand scaffolds were synthesized bearing large aryl (2,4,6-Ph₃C₆H₂, abbreviated Ar) or alkyl (^tBu, adamantyl) flanking groups to afford three new disubstituted ligands (^RL, 1,9-R₂-5-mesityldipyrrromethene, R = aryl, alkyl). While high-spin (*S* = 2), four-coordinate iron complexes of the type (^RL)FeCl(sol_v) were obtained with the alkyl-substituted ligand varieties (for R = ^tBu, Ad and sol_v = THF, OEt₂), use of the sterically encumbered aryl-substituted ligand precluded binding of solvent and cleanly afforded a high-spin (*S* = 2), three-coordinate complex of the type (^{Ar}L)FeCl. Reaction of (^{Ar}L)FeCl(OEt₂) with alkyl azides resulted in the catalytic amination of C–H bonds or olefin aziridination at room temperature. Using a 5% catalyst loading, 12 turnovers were obtained for the amination of toluene as a substrate, while greater than 85% of alkyl azide was converted to the corresponding aziridine employing styrene as a substrate. A primary kinetic isotope effect of 12.8(5) was obtained for the reaction of (^{Ar}L)FeCl(OEt₂) with adamantyl azide in an equimolar toluene/toluene-*d*₈ mixture, consistent with the amination proceeding through a hydrogen atom abstraction, radical rebound type mechanism. Reaction of *p*-^tBuC₆H₄N₃ with (^{Ar}L)FeCl permitted isolation of a high-spin (*S* = 2) iron complex featuring a terminal imido ligand, (^{Ar}L)FeCl(N(*p*-^tBuC₆H₄)), as determined by ¹H NMR, X-ray crystallography, and ⁵⁷Fe Mössbauer spectroscopy. The measured Fe–N_{imido} bond distance (1.768(2) Å) is the longest reported for Fe(imido) complexes in any geometry or spin state, and the disruption of the bond metrics within the imido aryl substituent suggests delocalization of a radical throughout the aryl ring. Zero-field ⁵⁷Fe Mössbauer parameters obtained for (^{Ar}L)FeCl(N(*p*-^tBuC₆H₄)) suggest a Fe^{III} formulation and are nearly identical with those observed for a structurally similar, high-spin Fe^{III} complex bearing the same dipyrrromethene framework. Theoretical analyses of (^{Ar}L)FeCl(N(*p*-^tBuC₆H₄)) suggest a formulation for this reactive species to be a high-spin Fe^{III} center antiferromagnetically coupled to an imido-based radical (*J* = –673 cm^{–1}). The terminal imido complex was effective for delivering the nitrene moiety to both C–H bond substrates (42% yield) as well as styrene (76% yield). Furthermore, a primary kinetic isotope effect of 24(3) was obtained for the reaction of (^{Ar}L)FeCl(N(*p*-^tBuC₆H₄)) with an equimolar toluene/toluene-*d*₈ mixture, consistent with the values obtained in the catalytic reaction. This commonality suggests the isolated high-spin Fe^{III} imido radical is a viable intermediate in the catalytic reaction pathway. Given the breadth of iron imido complexes spanning several oxidation states (Fe^{II}–Fe^V) and several spin states (*S* = 0 → 3/2), we propose the unusual electronic structure of the described high-spin iron imido complexes contributes to the observed catalytic reactivity.



I. INTRODUCTION

Introducing functionality into unactivated C–H bonds remains a significant challenge both in the realm of complex molecule synthesis as well as in the elaboration of simple hydrocarbon feedstocks into value-added commodity chemicals.^{1,2} Biological C–H bond functionalization is primarily performed by iron-containing enzymes that utilize dioxygen as the terminal oxidant. A key structural element of the putative hydroxylation catalyst in both heme (where iron is embedded in a porphyrin) and non-heme systems is a transiently formed terminal iron oxo species, typically thought to involve multiple-bond character.^{3,4} Furthermore, the reactivity of this intermediate is believed to be dictated by its electronic structure.^{5–7} In non-heme enzymes four such Fe^{IV}(oxo) complexes have been characterized, and their reactivity has been linked to a common electronic feature: namely a high-spin ground state (*S* = 2).⁴ However, an isolable, high-spin synthetic analogue has not

been reported that mimics the catalytic transfer of the metal–ligand multiply bonded functionality found in the biological systems.^{8–13}

Parallel to the work targeted at iron-mediated hydroxylation chemistry, C–H bond amination^{14–20} and olefin aziridination^{14,16,21–23} have been the focus of much recent synthetic work, although many mechanistic details and their interplay in effecting chemo- and regioselectivity remain poorly understood. The synthesis and characterization of Fe(imido) complexes as isoelectronic surrogates to Fe(oxo) functionalities have been targeted in the pursuit of effecting viable catalytic delivery of the nitrene functional unit to a C–H bond or olefinic substrates. Iron imido complexes have now been characterized in four oxidation states spanning a range of spin states (Fe^{II}, *S* = 0;²⁴

Received: November 18, 2010

Published: March 15, 2011

Scheme 1. Ligand and Metal Complex Syntheses

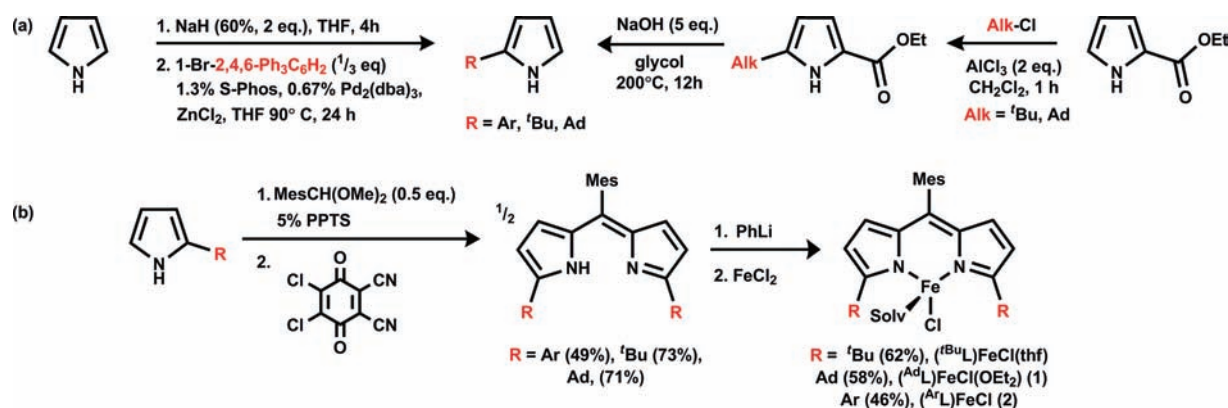


Table 1. Spectral and Magnetic Properties of Complexes 1–4

complex	μ_{eff} (μ_B)	S	λ/nm ($\epsilon/\text{M}^{-1} \text{cm}^{-1}$)	δ (mm/s) ^b	$ \Delta E_Q $ (mm/s) ^b
(^{tBu} L)FeCl(thf)	5.2(2)	2	497 (40 000) ^a		
(^{Ad} L)FeCl(OEt ₂) (1)	5.1(1)	2	494 (59 000) ^a	0.98	3.70
(^{Ar} L)FeCl (2)	5.1(2)	2	554 (26 000)	0.68	0.68
[(^{Ar} L)FeCl] ₂ (μ -N(Ph)(C ₆ H ₅)N) (3)	7.8(2)	5/2, 5/2	551 (27 000)	0.33	2.15
(^{Ar} L)FeCl(NC ₆ H ₄ -p-tBu) (4)	5.3(1)	2	553 (26 000)	0.29	2.29

^a UV/vis reported for pyridine adduct. ^b Recorded at 105 K.

Fe^{III}, $S = 1/2$, 1, $3/2$;^{25–30} Fe^{IV}, $S = 1$;^{31–33} Fe^V, $S = 1/2$ ³⁴) and have been shown to engage in group transfer to carbon monoxide to produce isocyanates^{25,35} and to isocyanides to produce carbodiimides,³⁵ undergo hydrogenation,²⁷ and perform H atom abstraction from C–H bonds.^{36,37} Herein we report room-temperature, catalytic C–H bond and olefin functionalization from a transiently formed, high-spin ($S = 2$) iron imido complex.

II. RESULTS AND DISCUSSION

During our investigations of iron dipyrromethene complexes as heme surrogates, we observed that reaction of an Fe^{II} complex with organic azides led to facile intramolecular delivery of the nitrene functional group into a ligand C–H bond.³⁷ The reaction was postulated to proceed via a high-valent Fe^{IV}(NR) species, akin to the hydroxylation pathway of cytochrome P450 and its functional analogues.^{38,39} Extending this reactivity to an intermolecular reaction required removal of reactive C–H bonds from the ligand platform. Thus, dipyrromethene platforms were targeted featuring sterically encumbered aryl or alkyl substituents that lack weak C–H bonds to circumvent intramolecular C–H bond activation pathways. Pyrroles substituted in the 2-position were afforded using modified Negishi coupling for 2-arylpyrroles and directed Friedel–Crafts alkylations for 2-alkylpyrroles. For example, 2,4,6-Ph₃-C₆H₂Br was cleanly coupled to sodium pyrrolide to afford 2-Ar(pyrrole) using conditions outlined by Sadighi and co-workers (3 equiv of sodium pyrrolide, 3 equiv of ZnCl₂, Pd₂(dba)₃ (0.67%)/S-Phos (1.33%); THF, 90 °C, 24 h, 84%; Ar = 2,4,6-Ph₃-C₆H₂; see Scheme 1a).⁴⁰ Alkyl-substituted pyrroles were synthesized in good yields by reaction of the corresponding alkyl chloride (R-Cl), AlCl₃, and ethyl pyrrole-2-carboxylate following decarboxylation (KOH, glycol, 200 °C, 12

h, R = adamantyl 88%, R = ^{tBu} 65%).^{41,42} Disubstituted dipyrromethene ligands (^XL, X = 1,9-substituent) were prepared using literature procedures to produce the ligands in good overall yields ((^{Ar}L)H, 49%; (^{tBu}L)H, 73%; (^{Ad}L)H, 71%; Scheme 1b).³⁷ Dipyrromethene deprotonation with phenyllithium in thawing benzene afforded the lithio species (^{Ar}L)Li, (^{tBu}L)Li, and (^{Ad}L)Li as brightly colored powders in nearly quantitative yields (88–92%) for subsequent transmetalation to iron (Scheme 1b).

Formation of the iron dipyrromethene complexes proceeds cleanly from reaction of the lithio dipyrromethene species with a thawing slurry of FeCl₂ in an ethereal solvent. For example, reaction of (^{Ad}L)Li with FeCl₂ in thawing diethyl ether cleanly affords the solvated complex (^{Ad}L)FeCl(OEt₂) (1) as a luminescent green-brown solid following precipitation (yield 58%; Scheme 1c). Utilizing the aryl-substituted ligand (^{Ar}L)Li under similar reaction conditions affords the three-coordinate species (^{Ar}L)FeCl (2) as a bright purple solid following crystallization (46%). The compositions and purity of 1 and 2 were established by ¹H NMR, UV–visible spectroscopy, ⁵⁷Fe Mössbauer spectroscopy, and combustion analysis, the data of which are compiled in Table 1. The respective geometries of four-coordinate 1 and three-coordinate 2 were verified by X-ray diffraction studies on a single crystal of each (Figure 1; see the Supporting Information). The solid-state molecular structure of 1 shows a trigonal-pyramidal geometry with a diethyl ether molecule capping the pyramid. Complex 2 has a trigonal-planar geometry about iron, wherein the large 2,4,6-Ph₃-C₆H₂ ligand substituents flank iron above and below the [N₂FeCl] plane. The average bond lengths of the four-coordinate complex (Fe–N_L = 2.035(4) Å, Fe–Cl = 2.249(1) Å) are expanded relative to three-coordinate species (Fe–N_L = 1.966(7) Å, Fe–Cl = 2.154(2) Å). The shorter bond lengths in the three-coordinate

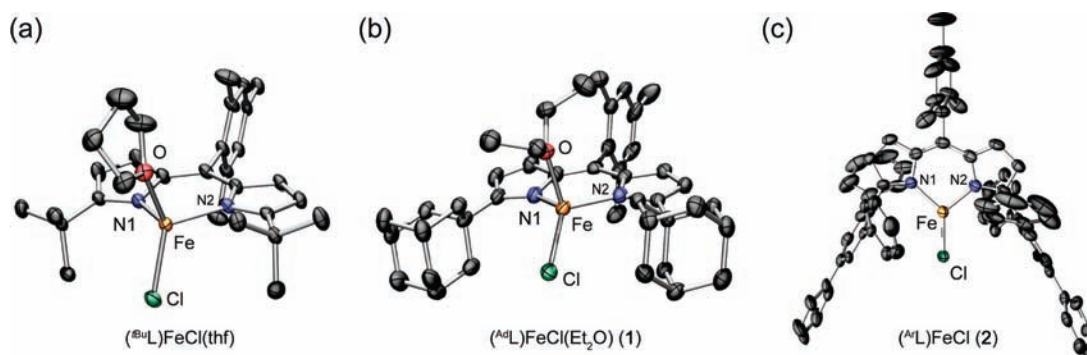


Figure 1. Solid-state molecular structures for (a) (${}^{t\text{Bu}}\text{L}$)FeCl(thf), (b) (${}^{\text{Ad}}\text{L}$)FeCl(OEt₂) (**1**), and (c) (${}^{\text{Ar}}\text{L}$)FeCl (**2**) with thermal ellipsoids at the 50% probability level. Color scheme: Fe, orange; Cl, green; C, black; N, blue. Hydrogens, solvent molecules, and aryl ring disorder in **2** are omitted for clarity. Bond lengths (Å) are as follows. (${}^{t\text{Bu}}\text{L}$)FeCl(thf): Fe–N1, 2.026(2); Fe–N2, 2.028(2); Fe–Cl, 2.255(1); Fe–O, 2.077(2). (${}^{\text{Ad}}\text{L}$)FeCl(OEt₂) (**1**): Fe–N1, 2.028(3); Fe–N2, 2.042(3); Fe–Cl, 2.250(2); Fe–O, 2.090(2). (${}^{\text{Ar}}\text{L}$)FeCl (**2**): Fe–N1, 1.966(5); Fe–N2, 1.966(5); Fe–Cl, 2.154(2).

Table 2. LC/MS (${}^1\text{H}$ NMR) Yields at Various Temperatures of Products Generated in Catalytic Amination Reaction with **1**

temp/°C	yield/ 10^{-2} mmol				TON
	BnAdNH	PhC(H)NAd	AdNH ₂	PhCH ₂ CH ₂ Ph	
25	6.5 (4.8)	0.19 (0.20)	0.12		6.7 (5.0)
60	9.8 (11)	0.19 (0.10)	0.46	(0.17)	10 (11)
90	8.1 (8.1)	0.58 (0.72)	2.1	(0.81)	8.7 (8.8)
120	5.7 (5.6)	0.29 (0.13)	1.6	(1.7)	6.0 (5.7)

species are likely a result of both decreased steric repulsion and the increased electrophilicity of iron in the absence of a fourth donor. The room-temperature solution magnetic moments determined using the method of Evans are 5.2(2) μ_{B} for **1** and 5.1(2) μ_{B} for **2**, both consistent with high-spin ($S = 2$) iron(II).⁴³ Zero-field ${}^{57}\text{Fe}$ Mossbauer analysis of **1** (δ , $|\Delta E_{\text{Q}}|$ (mm/s) 0.98, 3.70) and **2** (δ , $|\Delta E_{\text{Q}}|$ (mm/s) 0.67, 0.68) corroborate this assignment (see Table 1). The three-coordinate iron chloride **2** features an isomer shift lower than for the other four-coordinate dipyrromethene Fe^{II} complexes and a particularly small quadrupole splitting, though these unusual parameters are similar to those reported for structurally similar trigonal-planar, three-coordinate β -diketiminato complexes.⁴⁴

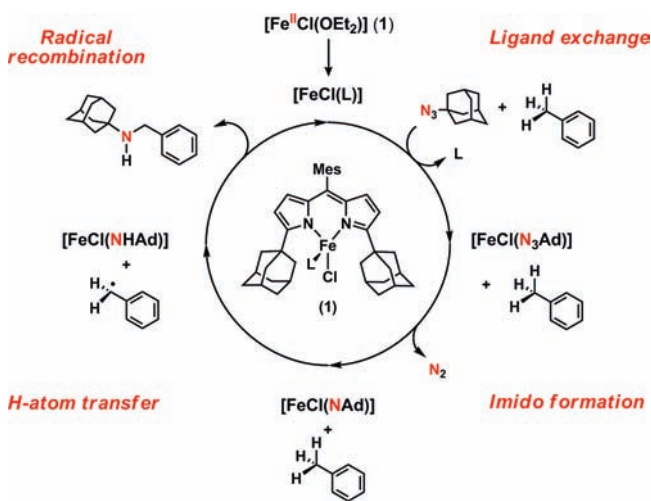
As the reaction of organic azides with (${}^{\text{Mes}}\text{L}$)FeCl(THF) gives rise to intramolecular amination of a ligand C–H bond,³⁷ we canvassed the reactivity of complex **1** with organic azides. When alkyl azides (e.g., (H_3C)₃CN₃, 1-azidoadamantane) are added to **1** in toluene, rapid azide consumption is evident and the product of intermolecular nitrene insertion into a benzylic C–H bond of toluene (PhCH₂NHR) is observed. Catalytic turnover is observed at room temperature when multiple equivalents of azide are used. Reactions of 1-azidoadamantane (N₃Ad) with **1** in toluene at room temperature yielded a mixture of benzyladamantylamine (95%), benzyladamantylimine (2.8%), and adamantylamine (1.8%) for a total of 6.7 turnovers (TON) (see Table 2). The turnover is maximized by running the reaction at 60 °C (TON = 10–12) but decreases substantially at elevated temperatures (TON: 8.7 at 90 °C; 6 at 120 °C). The ratios of the amination products change at elevated temperatures as well (at 120 °C: benzyladamantylamine (75%), benzyladamantylimine (4%), and adamantylamine (21%)). At elevated temperatures (60–120 °C) the presence of 1,2-diphenylethane (product of

coupling two PhCH₂^{*}) is also detectable by ${}^1\text{H}$ NMR. While elevated temperatures may facilitate amine dissociation from the iron catalyst, it does so at the expense of the thermal stability of the iron catalyst. Complex **1** is also effective for nitrene delivery to olefinic substrates. Near-quantitative nitrene transfer was observed when **1** is reacted with N₃Ad in styrene at room temperature, giving 85% of the corresponding aziridine (17 TON based on 20 equiv of azide).

Catalysis screens for the amination of toluene showed complex **1** to be the most active, whereas the *tert*-butyl analogue (${}^{t\text{Bu}}\text{L}$)FeCl(thf) only showed evidence for 5.6 turnovers at 60 °C, and complex **2** showed only trace amounts of aminated product by mass spectrometry. While THF found in the precatalyst (e.g., (${}^{\text{Ad}}\text{L}$)FeCl(thf)) is tolerated during catalysis, adding additional THF to the reaction suppresses amination. Addition of 5 equiv of THF to an amination reaction (20 equiv of N₃Ad/[**1**]) yields only 50% benzyladamantylamine with respect to the iron catalyst **1**. Addition of 50 equivalents of THF completely suppresses the reaction, as THF presumably outcompetes the azide from binding to the catalyst. Addition of a Lewis acid promoter (i.e., 1 equiv of B(C₆F₅)₃) to scavenge THF from the precatalyst did not increase the turnover observed for any of the precatalysts screened. Furthermore, the reaction is impeded by product inhibition. Addition of 10 equiv of adamantylamine or 15 equiv of benzyladamantylamine to **1** under typical catalytic conditions (5% **1**, toluene 60 °C) suppresses the catalytic amination to an undetectable amount.

The detection of 1,2-diphenylethane during the formation of benzyladamantylamine strongly suggests that an H atom abstraction pathway is operative. As a probe for direct H atom transfer, a competition experiment employing a 1:1 ratio of toluene to its perdeuterio analogue provides a kinetic isotope effect, $k_{\text{H}}/k_{\text{D}}$, of 12.8(5) for precatalyst **1**. The $k_{\text{H}}/k_{\text{D}}$ ratio is consistent with a C–H bond-breaking event contributing to the rate-determining step and the reaction proceeding by a hydrogen atom abstraction/rebound mechanism, as illustrated in Scheme 2. The observed KIE exceeds the values Che and co-workers reported for stoichiometric C–H amination from isolated Ru^{VI} bis-imido complexes (KIE: 4.8–11)^{45,46} and those reported by Warren and co-workers for nitrene delivery from a putative [Cu]₂(imido) complex (KIE: 5–6),⁴⁷ though the isotope effect reported for ethylbenzene amination by a Cu(amido) species is substantially higher (KIE: 70).⁴⁸ The large KIE value exceeds the classical value for hydrogen atom transfer (6.5)⁴⁹ and is thus suggestive of

Scheme 2. Proposed Catalytic Cycle for the Amination of C–H Bonds by Reaction of 1 with Organic Azides



H atom tunneling akin to that observed in TauD monooxygenases (KIE: 37)⁴ and several Fe^{IV}-oxo model complexes reported by Que and Nam (KIE: 18–50).^{11,50–52}

While our proposed mechanism suggests the intermediacy of an Fe^{IV} imido complex prior to the rate-determining step of H atom abstraction, we sought to validate this hypothesis via isolation or characterization of the putative intermediate. Reacting a thawing solution of **2** in benzene with a stoichiometric amount of phenyl azide quantitatively produces a ¹H NMR silent complex following consumption of the azide, as ascertained by the disappearance of the azide stretch (ν_{N_3}) by infrared spectroscopy. An X-ray diffraction study on crystals grown from the reaction mixture revealed the product to be the bimolecularly coupled species [(^{Ar}L)FeCl]₂(μ -N(Ph)(C₆H₅)N) (**3**), shown in Scheme 3, the solid-state molecular structure of which is shown in Figure 2a. The coupled product **3** presumably arises from radical coupling of two monomeric (^{Ar}L)FeCl(NPh) moieties to intermolecularly form a new N–C bond. Complex **3** features chemically distinct amide N(Ph)R ligation to one iron center (Fe2) and ketimide ligation to the second (Fe1). The (NPh) ketimide formulation is supported by the dearomatization of the C1–C6 ring, featuring localized double bonds (C2–C3 = 1.328(3) Å, C5–C6 = 1.331(3) Å, C1–N6 = 1.276(3) Å). The room-temperature magnetic moment for **3** is 7.8(2) μ_B , slightly lower than the calculated value of 8.3 μ_B for two noninteracting high-spin Fe^{III} centers ($S = 5/2$). The Fe^{III} formulation is corroborated by zero-field ⁵⁷Fe Mössbauer analysis of **3** at 100 K, which reveals that both iron centers in **3** have isomer shifts and quadrupole splitting parameters consistent with high-spin Fe^{III} (δ , $|\Delta E_Q|$ (mm/s) 0.33, 2.15). The parameters are significantly distinct from those of both the Fe^{II} precursor **2** (δ , $|\Delta E_Q|$ (mm/s) 0.68, 0.68) and the four-coordinate Fe^{II} species **1** (δ , $|\Delta E_Q|$ (mm/s) 0.98, 3.70) (Table 1).

In an effort to obtain a monomeric imido complex, **2** was reacted with *p*-^tBuC₆H₄N₃, where the aryl para substitution was selected to sterically prevent the radical coupling pathway observed in the formation of **3**.⁵³ In contrast to the dimerization observed in the reaction of **2** with phenyl azide, a new product from the reaction of **2** with *p*-^tBuC₆H₄N₃ is easily discernible by

¹H NMR as a C₂-symmetric species distinct from the starting material. The room-temperature magnetic moment for this species is 5.3(1) μ_B , consistent with an $S = 2$ complex. Zero-field ⁵⁷Fe Mössbauer analysis of the crude reaction product at 100 K reveals a single iron-containing species (δ , $|\Delta E_Q|$ (mm/s) 0.29, 2.29) that is nearly superimposable with the spectrum obtained for **3**, suggesting the new product also contains Fe^{III} (Figure 3a).

An X-ray diffraction study on single crystals grown from the reaction of **2** with *p*-^tBuC₆H₄N₃ revealed the product to be a monomeric species bearing a terminally bound imido ligand, (^{Ar}L)FeCl(NC₆H₄-*p*-^tBu) (**4**) (Figure 2b). The Fe–Cl (2.210(1) Å) and Fe–N_L (2.005(2) Å) bond lengths are consistent with those found in the bimolecularly coupled Fe^{III} dimer **3**. The Fe–N_{Ar} bond length in **4** (1.768(2) Å) is elongated relative to those in previously reported terminal imido complexes (e.g., [PhBP₃]Fe(N-tol) 1.658(2) Å, $S = 1/2$;²⁴ (^{Me}nacnac)Fe(NAd) 1.662(2) Å, $S = 3/2$;³⁰ (^{iPr}PDI)Fe(NAr) 1.705–1.717 Å, $S = 1$;²⁷ [(N4Py)Fe(NTs)]²⁺ 1.73 Å, $S = 1^{54}$), suggesting any iron–imido multiple-bond character is severely attenuated. To account for the anomalously long Fe–N_{Ar} bond length in **4**, the similar Mössbauer parameters for **3** and **4**, and the observed magnetic moment of monomeric **4**, we propose **4** is comprised of a high-spin Fe^{III} (d^5 , $S = 5/2$) center antiferromagnetically coupled to an imido-based radical ($S = 1/2$). The presence of an aryl-delocalized radical can be gleaned from the C–C bond distances within the nitrene aryl ring (N3–C1, 1.331(2) Å; C1–C2, 1.423(3) Å; C2–C3, 1.372(3) Å; C3–C4, 1.406(3) Å; C4–C5, 1.405(3) Å; C5–C6, 1.378(3) Å; C6–C1, 1.414(3) Å).⁵⁵ In comparison, for a para-substituted Fe^{III} imido species that does not feature radical character, the average bond distances within the imide aryl moiety are C–N = 1.383 Å, C_{ipso}–C_{ortho} = 1.401 Å, C_{ortho}–C_{meta} = 1.378 Å, and C_{meta}–C_{para} = 1.387 Å.²⁵ Probing the electronic structure by DFT corroborates the proposed electronic structure. Broken-symmetry calculations estimate the antiferromagnetic magnetic exchange coupling (J)⁵⁶ to be -673 cm^{-1} and the calculated Mössbauer parameters match well with those observed for **4** (calculated δ , $|\Delta E_Q|$ (mm/s) 0.34, -2.00).^{57,58} The calculated spin density plot ($\alpha - \beta$) for **4**, shown in Figure 3b, illustrates this exchange interaction.

Gratifyingly, monomeric **4** is a reactive source of arylnitrene. Complex **4** reacts rapidly with 1,4-cyclohexadiene to produce H₂N(C₆H₄-*p*-^tBu) and benzene, in addition to reacting with PMe₂Ph to produce the phosphinimide Me₂PhP=N(C₆H₄-*p*-^tBu) and **2**. Stirring **4** in toluene at room temperature produces the benzylic C–H amination product PhCH₂NH(C₆H₄-*p*-^tBu) (42% yield by ¹H NMR), where the remainder of the aryl azide is converted into the free aniline. The kinetic isotope effect for the putative imido species **4** was determined via a competition experiment employing a 1:1 ratio of toluene to its perdeuterio analogue, providing a kinetic isotope effect, k_H/k_D , of 24(3). While this value exceeds the kinetic isotope effect determined for precatalyst **1**, it is of the same order of magnitude and suggests complex **4** is representative of the transient group transfer reagent formed in the catalytic runs employing **1** as a precatalyst. Reacting **4** with styrene (200 equiv) at room temperature produces the aziridine Ph(CH₂)₂N(C₆H₄-*p*-^tBu) in good yield (76% by ¹H NMR). One competitive reaction pathway observed in the aziridination reaction is the radical polymerization of styrene initiated by **4**, though this could be minimized by dilution of the styrene substrate. In both the amination and

Scheme 3. Synthesis of the Bimolecularly Coupled Fe^{III} Imido Precursor **3** and the Terminal Imido Complex **4** with a Delocalized Imido-Based Radical, Fe^{III}([•]NAr), and Their Subsequent Reactivity with C–H Bonds

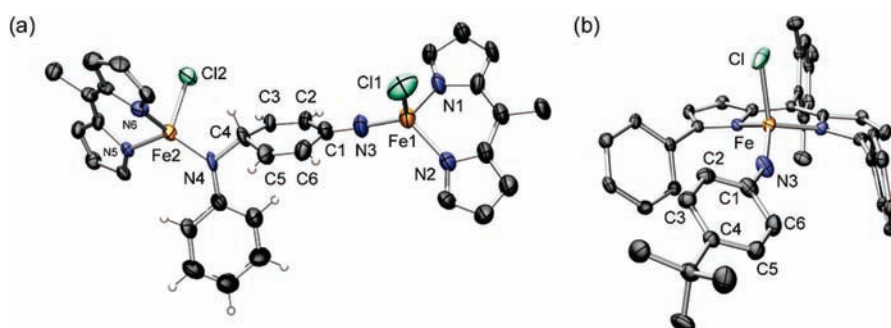
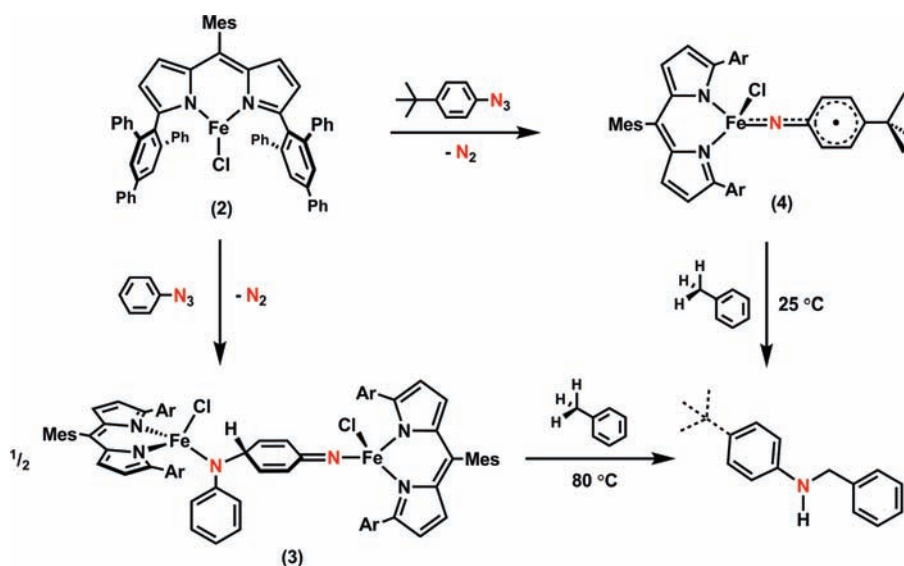


Figure 2. Solid-state core molecular structures for (a) **3** and (b) **4**. Ligand aryl substituents, hydrogen atoms, and solvent molecules are omitted for clarity. Bond lengths (Å) are as follows. For **3**: Fe1–N3, 1.810(2); Fe1–Cl1, 2.202(1); C1–N3, 1.276(3); C1–C2, 1.462(4); C2–C3, 1.328(3); C3–C4, 1.490(4); C4–C5, 1.489(4); C5–C6, 1.331(3); C6–C1, 1.462(4); N4–C4, 1.484(3); Fe2–Cl2, 2.228(1); Fe2–N4, 1.886(2). For **4**: Fe–Cl, 2.210(1); Fe–N3, 1.768(2); N3–Cl, 1.331(2); C1–C2, 1.423(3); C2–C3, 1.372(3); C3–C4, 1.406(3); C4–C5, 1.405(3); C5–C6, 1.378(3); C6–C1, 1.414(3).

aziridination reactions free amine, H₂NC₆H₄-*p*-^tBu, was observed by HR-MS, and **2** was formed as the predominant iron-containing product, as ascertained by ¹H NMR. Heating **4** in the presence of substrate leads to decreased yields of the corresponding amine and aziridine products. Traces of diazene (RN=NR) are also observable in the HR-MS of pure **4**, though how it forms remains unclear. Furthermore, dimeric **3** is also a reactive source of phenylnitrene, affording PhCH₂NHPh upon heating **3** in toluene to 80 °C (observed by HR-MS). Thus, dimeric **3** must be in equilibrium with its monomeric precursor, (^{Ar}L)FeCl(NPh), which reacts analogously to **4** to effect intermolecular C–H bond amination (Scheme 3).

Given the reactivity observed for **4**, we propose that an imido radical strongly coupled to a high-spin Fe^{III} ion, (L)Fe^{III}Cl([•]NR), is the putative group-transfer reagent in both the amination and aziridination catalytic processes. The reactive species reported herein is a departure from the typical Fe^{IV} assignment invoked in Fe-mediated group transfer catalysis.^{3,38,39} The isolation of the stable terminal imido radical **4** and the imido precursor **3** lend

support to this assignment. Reaction with alkyl azides in the catalytic reaction should localize the radical character on the imido N, giving rise to the observed enhanced reactivity toward C–H bond or olefinic substrates. We attribute the observed group transfer catalysis to the electronic structure, more specifically the localized radical character on the imido N, as the reactivity reported here is distinct from that of other Fe(imido) complexes.^{24–34,54,59} Metal imido complexes which bear radical character on the imido fragment have been invoked in other transition-metal complexes to explain the observed reactivity.^{47,60,61} Warren and co-workers invoke a terminal Cu^{III}(imido) species⁴⁷ and have demonstrated that a terminal Cu^{II}(amido) compound,⁴⁸ both of which are proposed to have radical character at N, are key intermediates in their C–H bond amination chemistry. A cobalt(III) imido species, reported by Theopold, which aminates an intramolecular C–H bond is also believed to have nitrogen radical character at room temperature despite a diamagnetic ground state.⁶² Thus, while the terminal imido radical bound to a ferric center (**4**) is the first example of an

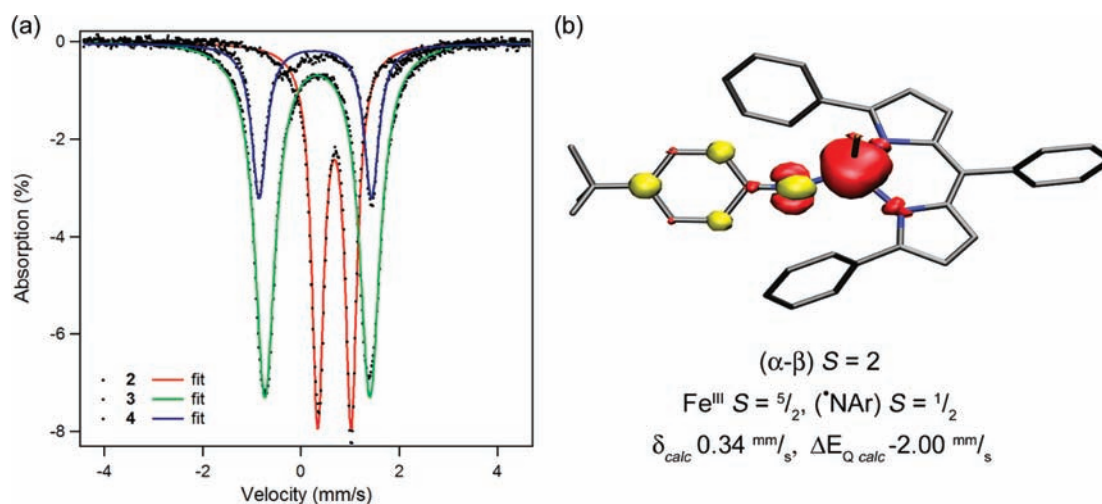


Figure 3. Terminal imido radical complex **4** exhibiting Mössbauer metrical parameters nearly identical with those of the bimolecularly coupled diferric **3**, illustrated in (a) by the zero-field 100 K ^{57}Fe Mössbauer spectral data, presented as black dots with spectral fits as solid lines (δ , $|\Delta E_Q|$ (mm/s)): Fe^{II} **2** (red) 0.68, 0.68; $(\text{Fe}^{\text{III}})_2$ **3** (green) 0.33, 2.15; $\text{Fe}^{\text{III}}(*\text{NAr})$ **4** (blue) 0.29, 2.29) and antiferromagnetic coupling between the high-spin Fe^{III} ion with the terminal imido radical in **4**, illustrated in (b) by the calculated spin density population ($\alpha - \beta$) for **4** ($S = 2$) by DFT (B3LYP/TZVP, SV(P); ORCA 2.7⁵⁸).

isolated complex featuring this type of high-spin electronic configuration, the electronic structure may arise in other synthetic and biochemical catalytic cycles.^{4,7,63–66}

III. CONCLUSIONS

Catalytic C–H bond amination and olefin aziridination have been observed from the reaction of organic azides with a simple iron(II) coordination complex supported by dipyrromethene ligands. Kinetic isotope analysis of the amination reaction suggests the C–H bond-breaking event contributes to the rate-limiting step of the reaction, followed by a radical rebound. Isolation of a reactive intermediate reveals the putative nitrene-delivery precursor to be a high-spin ($S = 2$) iron complex featuring a terminal imido ligand. Crystallographic, spectroscopic, and theoretical analyses suggest a formulation for this reactive species to be a high-spin iron(III) center antiferromagnetically coupled to an imido-based radical. The terminal imido complex was effective for delivering the nitrene moiety to both the C–H bond and olefinic substrates. The similarities observed in the kinetic isotope effects observed during catalytic runs and those using the isolated imido suggest the high-spin Fe^{III} (imido radical) is representative of the group transfer reagent in the catalytic sequence. Given the breadth of iron imido complexes spanning several oxidation states ($\text{Fe}^{\text{II}}\text{--}\text{Fe}^{\text{V}}$) and several spin states ($S = 0 \rightarrow 3/2$), we propose that the unusual electronic structure of the described high-spin iron imido complexes contributes to the observed catalytic reactivity. The high-spin nature and radical nitrene character serve to destabilize the Fe–imido bond, which presumably leads to the observed reactivity. Work is currently underway to determine the generality and scope of the nitrene-transfer reaction and to find whether this group transfer reaction pathway is amenable for the delivery of other functional groups.

■ ASSOCIATED CONTENT

S Supporting Information. Text, figures, tables, and CIF files giving details of the syntheses of **1–4**, reactivity and catalysis experiments for **1–4**, Mössbauer spectra and parameters for **1–**

4, selected bond lengths for **1–4**, solid-state structures for **1–4**, crystallographic data for **1–4**, and a description of computational methods and calculated molecular orbitals for **4**. This material is available free of charge via the Internet at <http://pubs.acs.org>.

■ AUTHOR INFORMATION

Corresponding Author

*E-mail: betley@chemistry.harvard.edu.

■ ACKNOWLEDGMENT

We thank Harvard University, the ACS PRF Fund (Type G), and the NSF (CHE-0955885) for financial support and Prof. R. H. Holm for the generous use of his Mössbauer spectrometer. E. T.H. thanks the DOE SCGF for a predoctoral fellowship. We thank Dr. Andrew Tyler for help with GC and LCMS studies.

■ REFERENCES

- (1) Bergman, R. G. *Nature* **2007**, *446*, 391.
- (2) Labinger, J. A.; Bercaw, J. E. *Nature* **2002**, *417*, 507.
- (3) Ortiz de Montellano, P. R.; Ed. *Cytochrome P450: Structure, Mechanism, and Biochemistry*, 4th ed.; Kluwer Academic/Plenum Publishers: New York, 2005.
- (4) Krebs, C.; Fujimori, D. G.; Walsh, C. T.; Bollinger, M. J., Jr. *Acc. Chem. Res.* **2007**, *40*, 484.
- (5) Decker, A.; Rhode, J.-U.; Klinker, E. J.; Wong, S. D.; Que, L., Jr.; Solomon, E. I. *J. Am. Chem. Soc.* **2007**, *129*, 15938.
- (6) Bernasconi, L.; Louwerse, M. J.; Baerends, E. J. *Eur. J. Inorg. Chem.* **2007**, 3023.
- (7) Ye, S.; Neese, F. *Curr. Opin. Chem. Biol.* **2009**, *13*, 89.
- (8) Pestovsky, O.; Stoian, S.; Bominaar, E. M.; Shan, X.; Münck, E.; Que, L., Jr.; Bakac, A. *Angew. Chem., Int. Ed.* **2005**, *44*, 6871.
- (9) Kaizer, J.; Klinker, E. J.; Oh, N. Y.; Rhode, J.-U.; Song, W. J.; Stubna, A.; Kim, J.; Münck, E.; Nam, W.; Que, L., Jr. *J. Am. Chem. Soc.* **2004**, *126*, 472.
- (10) Kumar, D.; Hirao, H.; Que, L., Jr.; Shaik, S. *J. Am. Chem. Soc.* **2005**, *127*, 8026.
- (11) England, J.; Martinho, M.; Farquhar, E. R.; Frisch, J. R.; Bominaar, E. L.; Münck, E.; Que, L., Jr. *Angew. Chem., Int. Ed.* **2009**, *48*, 3622.

- (12) England, J.; Guo, Y.; Farquhar, E. R.; Young, V. G., Jr.; Münck, E.; Que, L., Jr. *J. Am. Chem. Soc.* **2010**, *132*, 8635.
- (13) Lacy, D. C.; Gupta, R.; Stone, K. L.; Greaves, J.; Ziller, J. W.; Hendrich, M.; Borovik, A. S. *J. Am. Chem. Soc.* **2010**, *132*, 12188.
- (14) Müller, P.; Fruit, C. *Chem. Rev.* **2003**, *103*, 2905.
- (15) Davies, H. M. L.; Long, M. S. *Angew. Chem., Int. Ed.* **2005**, *44*, 3518.
- (16) Halfen, J. A. *Curr. Org. Chem.* **2005**, *9*, 657.
- (17) Cenini, S.; Gallo, E.; Caselli, A.; Ragaini, R.; Fantauzzi, S.; Piangiolino, C. *Coord. Chem. Rev.* **2006**, *250*, 1234.
- (18) Davies, H. M. L.; Manning, J. R. *Nature* **2008**, *451*, 417.
- (19) Collet, F.; Dodd, R. H.; Dauban, P. *Chem. Commun.* **2009**, 5061.
- (20) Zalatan, D. N.; Du Bois, J. *Top. Curr. Chem.* **2010**, *292*, 347.
- (21) Tanner, D. *Angew. Chem., Int. Ed.* **1994**, *33*, 599.
- (22) Osborn, H. M. I.; Sweeney, J. B. *Tetrahedron: Asymmetry* **1997**, *8*, 1693.
- (23) Sweeney, J. B. *Chem. Soc. Rev.* **2002**, *31*, 247.
- (24) Brown, S. D.; Peters, J. C. *J. Am. Chem. Soc.* **2005**, *127*, 1913.
- (25) Brown, S. D.; Betley, T. A.; Peters, J. C. *J. Am. Chem. Soc.* **2003**, *125*, 322.
- (26) Betley, T. A.; Peters, J. C. *J. Am. Chem. Soc.* **2003**, *125*, 10782.
- (27) Bart, S. C.; Lobkovsky, E.; Bill, E.; Chirik, P. J. *J. Am. Chem. Soc.* **2006**, *128*, 5302.
- (28) Lu, C. C.; Saouma, C. T.; Day, M. W.; Peters, J. C. *J. Am. Chem. Soc.* **2007**, *129*, 4.
- (29) Scepaniak, J. J.; Young, J. A.; Bontchev, R. P.; Smith, J. M. *Angew. Chem., Int. Ed.* **2009**, *48*, 3158.
- (30) Cowley, R. E.; DeYonker, N. J.; Eckert, N. A.; Cundari, T. R.; DeBeer, S.; Bill, E.; Ottenwaelder, X.; Flaschenriem, C.; Holland, P. L. *Inorg. Chem.* **2010**, *49*, 6172.
- (31) Verma, A. K.; Nazif, T. N.; Achim, C.; Lee, S. C. *J. Am. Chem. Soc.* **2000**, *122*, 11013.
- (32) Thomas, C. M.; Mankad, N. P.; Peters, J. C. *J. Am. Chem. Soc.* **2006**, *128*, 4956.
- (33) Nieto, I.; Ding, R.; Bontchev, R. P.; Wang, H.; Smith, J. M. *J. Am. Chem. Soc.* **2008**, *130*, 2716.
- (34) Ni, C.; Fettinger, J. C.; Long, G. J.; Brynda, M.; Power, P. P. *Chem. Commun.* **2008**, 6045.
- (35) Cowley, R. E.; Eckert, N. A.; Elhaik, J. E.; Holland, P. L. *Chem. Commun.* **2009**, 1760.
- (36) Cowley, R. E.; Holland, P. L. *Inorg. Chim. Acta* **2011**, in press.
- (37) King, E. R.; Betley, T. A. *Inorg. Chem.* **2009**, *48*, 2361.
- (38) Groves, J. T. *J. Chem. Educ.* **1985**, *62*, 928.
- (39) Sono, M.; Roach, M. P.; Coulter, E. D.; Dawson, J. H. *Chem. Rev.* **1996**, *96*, 2841.
- (40) Rieth, R. D.; Mankad, N. P.; Calimano, E.; Sadighi, J. P. *Org. Lett.* **2004**, *6*, 3981.
- (41) Bailey, D. M.; Johnson, R. E.; Albertson, N. F. *Organic Syntheses*; Wiley: New York, 1988; Collect Vol. 6, 618.
- (42) Harman, W. H.; Harris, T. D.; Freedman, D. E.; Fong, H.; Chang, A.; Rinehart, J. D.; Ozarowski, A.; Sougrati, M. T.; Grandjean, F.; Long, G. L.; Long, J. R.; Chang, C. J. *J. Am. Chem. Soc.* **2010**, *132*, 18115.
- (43) Evans, D. F. *J. Chem. Soc.* **1959**, 2003.
- (44) Andres, H.; Bominaar, E. L.; Smith, J. M.; Eckert, N. A.; Holland, P. L.; Münck, E. *J. Am. Chem. Soc.* **2002**, *124*, 3012.
- (45) Au, S. M.; Huang, J. S.; Yu, W. Y.; Fung, W. H.; Che, C. M. *J. Am. Chem. Soc.* **1999**, *121*, 9120.
- (46) Leung, S. K. Y.; Tsui, W. M.; Huang, J. S.; Che, C. M.; Liang, J. L.; Zhu, N. Y. *J. Am. Chem. Soc.* **2005**, *127*, 16629.
- (47) Badiei, Y. M.; Dinescu, A.; Dai, X.; Palomino, R. M.; Heinemann, F. W.; Cundari, T. R.; Warren, T. H. *Angew. Chem., Int. Ed.* **2008**, *47*, 9961.
- (48) Wiese, S.; Badiei, Y. M.; Gephart, R. T.; Mossin, S.; Varonka, M. S.; Melzer, M. M.; Meyer, K.; Cundari, T. R.; Warren, T. H. *Angew. Chem., Int. Ed.* **2010**, *49*, 8850.
- (49) Anslyn, E. V.; Dougherty, D. A. In *Modern Physical Organic Chemistry*; University Science Books: Sausalito, CA, 2006.
- (50) Que, L., Jr. *Acc. Chem. Res.* **2007**, *40*, 493.
- (51) Nam, W. *Acc. Chem. Res.* **2007**, *40*, 522.
- (52) Klinker, E. J.; Shaik, S.; Hirao, H.; Que, L., Jr. *Angew. Chem., Int. Ed.* **2009**, *48*, 1291.
- (53) Peters and co-workers reported a Cu di-*p*-tolyl aminyl radical, in which the tolyl methyl groups prevented radical coupling to form aryl-aryl-linked dimers, which were seen if methyl was replaced with hydrogen by using a diphenyl amido unit. See: Mankad, N. P.; Antholine, W. E.; Szilagy, R. K.; Peters, J. C. *J. Am. Chem. Soc.* **2009**, *131*, 3878.
- (54) Klinker, E. J.; Jackson, T. A.; Jensen, M. P.; Stubna, A.; Juhász, G.; Bominaar, E. L.; Münck, E.; Que, L., Jr. *Angew. Chem., Int. Ed.* **2006**, *45*, 7394.
- (55) Chaudhuri, P.; Verani, C. N.; Bill, E.; Bothe, E.; Weyhermüller, T.; Wieghardt, K. *J. Am. Chem. Soc.* **2001**, *123*, 2213.
- (56) With spin Hamiltonian $H = -2J_{\text{Fe}} \cdot S_{\text{NR}}$ and coupling constant $J = -(E_{\text{HS}} - E_{\text{BS}}) / (\langle S^2 \rangle_{\text{HS}} - \langle S^2 \rangle_{\text{BS}})$.
- (57) Ye, S.; Tuttle, T.; Bill, E.; Simkhovich, L.; Gross, Z.; Thiel, W.; Neese, F. *Chem. Eur. J.* **2008**, *14*, 10839.
- (58) Neese, F. *ORCA-An ab initio, Density Functional and Semi-empirical Electronic Structure Package, Version 2.7-00 ed.*; Universität Bonn, Bonn, Germany, 2009.
- (59) Mankad, N. P.; Müller, P.; Peters, J. C. *J. Am. Chem. Soc.* **2010**, *132*, 4083.
- (60) Lu, C. C.; DeBeer George, S.; Weyhermüller, T.; Bill, E.; Bothe, E.; Wieghardt, K. *Angew. Chem., Int. Ed.* **2008**, *47*, 6384.
- (61) Kogut, E.; Wiencko, H. L.; Zhang, L.; Cordeau, D. E.; Warren, T. H. *J. Am. Chem. Soc.* **2005**, *127*, 11248.
- (62) Shay, D. T.; Yap, G. P. A.; Zakharov, L. N.; Rheingold, A. L.; Theopold, K. H. *Angew. Chem., Int. Ed.* **2005**, *44*, 1508.
- (63) Groves, J. T.; Van Der Puy, M. *J. Am. Chem. Soc.* **1974**, *96*, 5274.
- (64) Groves, J. T.; McClusky, G. A. *J. Am. Chem. Soc.* **1976**, *98*, 859.
- (65) Chen, M. S.; White, M. C. *Science* **2007**, *318*, 783.
- (66) Chen, M. S.; White, M. C. *Science* **2010**, *327*, 566.